Title

Trajectory Design And Implementation Of Longitudinal Maneuvers On AHS Automated And Transition Lanes

Authors

Chen, Pin-yen
Alvarez, Luis
Horowitz, Roberto

Publication Date

1997

CALIFORNIA PATH PROGRAM
INSTITUTE OF TRANSPORTATION STUDIES
UNIVERSITY OF CALIFORNIA, BERKELEY

Trajectory Design and Implementation of Longitudinal Maneuvers on AHS Automated and Transtion Lanes

Pin-Yen Chen, Luis Alvarez, Roberto Horowitz
University of California, Berkeley

California PATH Research Report
UCB-ITS-PRR-97-49

This work was performed as part of the California PATH Program of the University of California, in cooperation with the State of California Business, Transportation, and Housing Agency, Department of Transportation; and the United States Department of Transportation, Federal Highway Administration.

Report for MOU 238

November 1997

ISSN 1055-1425

Trajectory Design and Implementation of Longitudinal Maneuvers on AHS Automated and Transition Lanes[1]

Pin-Yen Chen[2]
Luis Alvarez[3]
Roberto Horowitz[4]

Department of Mechanical Engineering
University of California at Berkeley
Berkeley CA 94720-1740

November 6, 1997

[1]Research supported by UCB-ITS PATH grants MOU-238 and MOU-287.
[2]Graduate student. Currently at Measurex Corporation. Email: `Chen_pin-Yen@measurex.com`.
[3]Postdoctoral researcher. Email: `alvar@scorpio.me.berkeley.edu`.
[4]Professor. Email: `horowitz@me.berkeley.edu`.

Abstract

A modification to the safe trajectory proposed in (Li et al., 1997) for the regulation layer maneuvers in the PATH AHS hierarchical architecture in (Varaiya and Shadlover, 1991) is proposed. The new design relies in a more conservative behavior for the trail platoon and allows to avoid even low speed collisions in the maneuvers for most of the cases. Only disturbances that occur when platoons are close to each other may produce collisions, although these collisions always have relative velocities that are below the given safety threshold. Explicit constraints for the splining between the regions of the safety curves are also imposed in order to guarantee comfort under normal conditions. The price for the higher degree of safety is tolled in extra completion time. The new design is applied to the *join* maneuver in the normal mode of operation, to the *frontdock* maneuver in degraded mode and also to the *stoplight* maneuver in the entry lane. In order to achieve zero-acceleration at the end of this maneuver, a finishing curve which is dynamic to the acceleration of the object platoon is proposed. Simulation results are presented and performance analyses are made.

Keywords

Automated highway systems, platooning, safe trajectories, join, entry and stoplight maneuvers.

Acknowledgements

This research is part of a larger group effort to develop control systems for AHS in degraded mode and faulty conditions of operation. Besides the authors, this group consist of Prof. Shankar Sastry, Prof. Pravin Varaiya, Dr. Raja Sengupta, Dr. Datta Godbole, Dr. John Lygeros, Jason Carbaugh, Tony Lindsey, John Haddon and other graduate students. Their input to this work is gratefully acknowledged.

Executive Summary

In this report we present a modification to the safe trajectory proposed in (Li et al., 1997) for the regulation layer maneuvers of the hierarchical PATH AHS architecture. This new design relies in a more conservative behavior for the controlled platoon in a maneuver. The new trajectory design avoids even low speed collisions for most of the cases. Only disturbances that occur when platoons are close to each other may produce collisions, although this collisions have always a relative velocity below the given safety threshold. Explicit constraints for the splining between the regions of the safety trajectory are also imposed in order to guarantee comfort under normal conditions. The price for the higher degree of safety is tolled in extra completion time for the maneuvers.

This new design is applied to the *join* maneuver in the normal mode of operation, the *frontdock* maneuver in degraded mode and also to the *stoplight* maneuver in the entry lane. In order to achieve zero-acceleration at the end of this maneuver, a finishing curve which is dynamic to the acceleration of the object platoon is proposed. The controller proposed in (Li et al., 1997) is used in the three maneuvers. Simulation results obtained in SmartPath and with an ad-hoc simulation tool are presented.

For a vehicle in an entry transition lane executing the *stoplight* maneuver, the extra time for completion is small. This increase is acceptable because the normal behavior for an entry vehicle will be that of joining a vehicle in front which continually varies its acceleration; frequent stopping is also common in this case. For the *join* maneuver in the normal mode of operation the increase of time for completion is relatively larger and therefore will have a greater impact on the highway throughput.

Contents

List of Figures

Chapter 1

Introduction

Under the Automated Highway System (AHS) architecture proposed by (Varaiya and Shadlover, 1991) in the California PATH project (see Fig. 1.1), automated vehicles would travel in"platoons" of closely spaced vehicles in automated lanes. The tight spacing between vehicles within a platoon prevents collisions at high relative velocities. The gap between two platoons on the other hand is arranged to be large enough so that the trail platoon would have time to stop even if the lead platoon brakes abruptly.

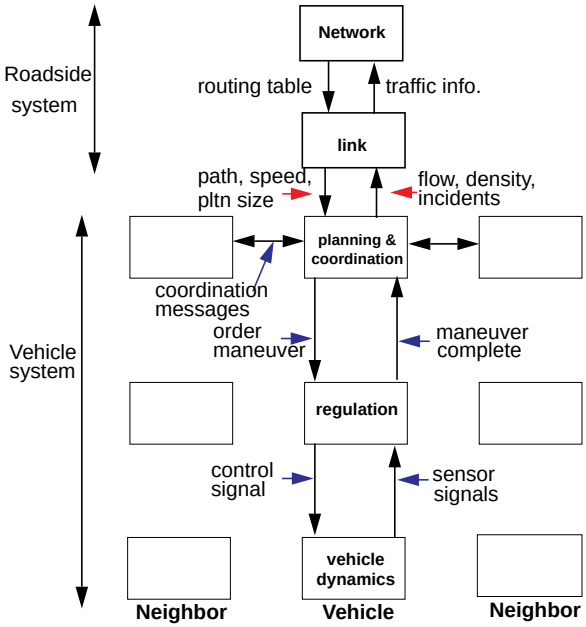

Figure 1.1: PATH AHS hierarchical architecture.

For the normal mode of operation, a hierarchical control architecture was proposed in (Hsu et al., 1991; Varaiya, 1993). This control architecture was later extended to the degraded modes of operation, that allow the system to function under adverse environmental conditions and system failures, in (Lindesy, 1996; Lygeros et al., 1995). There is a set of maneuvers designed to coordinate the motion of platoons in the highway, for each control architecture.

Among all the regulation layer maneuvers defined in (Hsu et al., 1991; Lygeros et al., 1995), those who involve closing up a gap between two platoons are of the most risk. The reason is that in such maneuvers one platoon is moving much faster (or slower) than the other, while the distance for reacting to a sudden deceleration or acceleration is being shortened. Such maneuvers include the *join* in the normal mode, and the *frontdock* in the degraded mode. Using the assumption that a platoon in the AHS architecture in (Varaiya and Shadlover, 1991) can be involved only in one maneuver at a time, one of the two platoons involved in these maneuvers would either cruise at a constant speed (or should be attempting to maintain it), unless an emergency happens. In other words, a closing gap maneuvers would generally be performed with one of the two platoons having no acceleration.

In (Li et al., 1997) safe control laws were proposed for AHS platoon leaders. The notion of a safety region was introduced and a generic controller was designed for the normal mode of operation control laws. This controller guarantees the safety and time optimality for the maneuvers on the automated lanes. The design approach can be easily extended to fault handling maneuvers in the degraded mode of operation with little modifications.

For maneuvers on the transition lane (Godbole et al., 1995), however, special care has to be taken since these maneuvers should be performed with all platoons having different accelerations. One example is the *stoplight* maneuver which is a necessary for organizing the entrance of vehicles into the automated lanes. Under the entry/exit design in (Godbole et al., 1995), a manually driven vehicle becomes an automatically driven vehicle after it passes through a check station. The vehicle starts to execute the *stoplight* maneuver in the stop-light zone until it comes to a stop either behind another car or at the stop light. All vehicles are operating as one car platoons, or "free agents", under this maneuver. The behavior of vehicles in the stop-light zone resembles that of a queue. The existence of this queue introduces a new set of constraints into the trajectory design:

- The velocity at which the *stoplight* maneuver operates is lower than that of the maneuvers on the automated lane.
- There are two desired velocity trajectories: one is calculated with respect to the stop light, the other is calculated with respect to the vehicle immediately in front. The decision on which one to choose depends on the relative distances to the stop light and the vehicle in front.
- The desired trajectory that the vehicle follows when it is in the queue should bring a vehicle to a full stop, without the need of switching into another control law.
- The maneuver should not allow any collision when a vehicle approach another vehicle in front which has a continually varying acceleration.

In this report, we present a modified *join* trajectory which is more conservative than that which was derived in (Li et al., 1997). This new trajectory reduces the chance of having a collision when the platoon ahead applies and holds maximum braking. Moreover, cars which follow this new trajectory will finish their maneuvers with zero acceleration and jerk. The proposed trajectory is used with the controller proposed in (Li et al., 1997).

The new trajectory proposed in this report is also applied to other maneuvers on the automated lanes, such as the *stoplight* in normal mode and the *frontdock* in degraded mode with no or little modification. Higher degree of safety and the inherent zero-acceleration ending condition are the major advantages over the current designs (Li et al., 1997; Lindesy, 1996). This results in a further decrease in the probability of a collision when safety is compromised and a perfect "lock-up" at the end of the maneuver. However, these improvements are tolled in terms of extra completion time. In the cases where time of completion is critical, these trajectories may not be convenient.

In Chapter 2, we discuss the concepts of safety and safety region for a maneuver. In Chapter 3, a trajectory design which is capable of addressing issues associated with the *stoplight* maneuver is proposed. In Chapter 4, we discuss the implementations of *join*, *stoplight* and *frontdock* maneuver with the proposed trajectory design; all of the controllers are implemented in SmartPath (Eskafi et al., 1992), the highway simulator of the California PATH project. Simulation results are shown in Chapter 5. Concluding remarks in are presented in Chapter 6.

Chapter 2

Safe Maneuvers

Safety is the major issue when vehicles perform maneuvers. In this chapter, we briefly review the definitions of safety and safe control as proposed in (Frankel et al., 1994; Li et al., 1997). Subsequently, we describe a region in the maneuver's state space such that when the trajectory of a maneuver is kept within this safety region it can be executed safely. Properties of this safety boundary are explored and illustrated.

2.1 Definitions of safety and safety region

The notion of safe AHS maneuvers was first introduced in (Frankel et al., 1994), where safety was defined as the absence of collisions with a relative velocity greater than a given threshold. Analysis on conditions for safe maneuvering of vehicles on an automated highway was realized in (Li et al., 1997) under the following three assumptions:

1. All vehicles have the same braking and acceleration capabilities, i.e. the acceleration of any vehicle lies in the range of $[-a_{min}, a_{max}]$.

2. No reverse motion is allowed on the automated highway.

3. If a vehicle is applying maximum acceleration, a_{max}, the maximum deceleration, $-a_{min}$, can be achieved after d seconds of delay from the time the full braking command is issued.

In this section we reproduce the definitions of *unsafe impact* and *safe control law* and a theorem for the safety of control laws stated in (Li et al., 1997).

Consider two platoons traveling on the automated highway as shown in Fig. 2.1, the trail platoon is moving behind the lead platoon in the same lane. Let $x_{trail}(t)$ and $x_{lead}(t)$ be the positions of the leader of the trail platoon and the last vehicle of the lead platoon at time t, and let $\dot{x}_{trail}(t)$, $\dot{x}_{lead}(t)$, $\ddot{x}_{trail}(t)$, and $\ddot{x}_{lead}(t)$ denote their first and second time derivatives respectively[1]. Let $w(t)$ be the acceleration of the lead platoon and $u(t)$ be that of the trail platoon.

[1] $\dot{x}_{lead}(t)$ and $\dot{x}_{trail}(t)$ will also be denoted by $v_{lead}(t)$ and $v_{trail}(t)$.

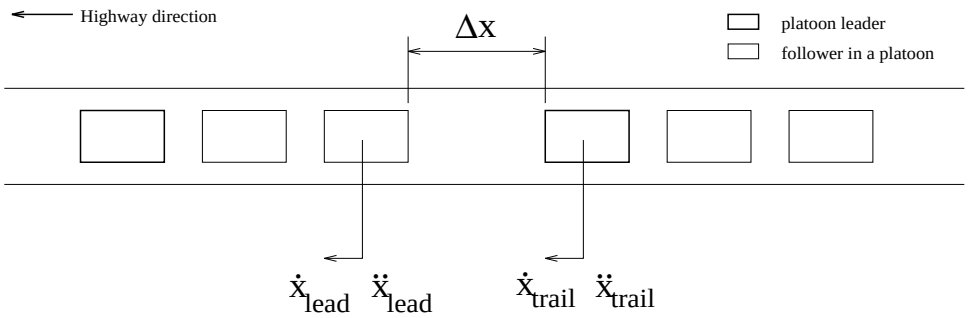

Figure 2.1: Notation for two platoons on the highway.

After applying an input/output linearization procedure to the dynamic model of a vehicle as in (Swaroop, 1994), the dynamics of the platoons become

$$\ddot{x}_{lead}(t) = w(t)\,, \tag{2.1}$$
$$\ddot{x}_{trail}(t) = u(t)\,, \tag{2.2}$$

where $w(t),\ u(t) \in [-a_{min}, a_{max}]$ for all time t.

We are interested on analyzing collisions between the lead and the trail vehicles in Fig. 2.1. As the relevant dynamics for collision are independent of the absolute positions, x_{lead} and x_{trail}, define the relative distance between the platoons to be

$$\Delta x(t) = x_{lead}(t) - x_{trail}(t)\,. \tag{2.3}$$

The dynamics of the relative motion between the lead and trail platoons is given by

$$\Delta\dot{x}(t) = \dot{x}_{lead}(t) - \dot{x}_{trail}(t)\,, \tag{2.4}$$
$$\Delta\ddot{x}(t) = \ddot{x}_{lead}(t) - \ddot{x}_{trail}(t) = w(t) - u(t)\,, \tag{2.5}$$
$$\dot{v}_{lead}(t) = w(t)\,, \tag{2.6}$$

where $\Delta\dot{x}(t)$ and $\Delta\ddot{x}(t)$ denote the relative velocity and relative acceleration between the platoons. Eq. (2.6) is necessary to account for the independence of $w(t)$ and $u(t)$.

Definition 2.1 (Unsafe impact) *An unsafe impact is said to happen at time t if*

$$\Delta x(t) \leq 0 \text{ and } -\Delta\dot{x}(t) \geq v_{allow}\,, \tag{2.7}$$

with $v_{allow} \geq 0$ being the maximum allowable relative impact velocity.

The notation $X_{MS} \subset R^3$ is used to denote the set of all triples $(\Delta x, \Delta\dot{x}, v_{lead})$ where $v_{lead} \geq 0$ and inequalities (2.7) are not satisfied. Notice that $(\Delta x(t), \Delta\dot{x}(t), v_{lead}(t)) \in X_{MS}$ for a given t, does not guarantee that $(\Delta x(t_1), \Delta\dot{x}(t_1), v_{lead}(t_1)) \in X_{MS}$ for $t_1 > t$. We are interested in finding a subset of X_{MS} such that this condition can be guaranteed for any admisable behavior of the lead vehicle.

Definition 2.2 (Safe Control) *A control law for the trail platoon $u(t)$ is said to be safe for an initial condition $(\Delta x(0), \Delta\dot{x}(0), v_{lead}(0))$, if for $v_{lead} \geq 0$ and any arbitrary lead platoon acceleration $\ddot{x}_{lead} = w(\tau)$, where $w(\tau) \in [-a_{min}, a_{max}]$ for $\tau \geq 0$, $(\Delta x(t), \Delta\dot{x}(t), v_{lead}(t)) \in X_{MS}$ for all $t \geq 0$.*

Theorem 2.1 *Let $X_{safe} \subset R^3$ be the set of $(\Delta x, \Delta\dot{x}, v_{lead})$ that satisfy:*

$$-\Delta\dot{x} < \max \begin{cases} -(a_{max} + a_{min})d - v_{lead} \\ \quad +\sqrt{2a_{min}\Delta x + v_{lead}^2 + v_{allow}^2 + a_{min}(a_{max} + a_{min})d^2}, \\ -(a_{max} + a_{min})d + v_{allow}\ . \end{cases} \tag{2.8}$$

There exists a control law that is safe for any initial condition $(\Delta x(0), \Delta\dot{x}(0), v_{lead}(0)) \in X_{safe}$, in the sense of Definition (2.2). Moreover, any control law that applies maximum braking whenever $(\Delta x(t), \Delta\dot{x}(t), v_{lead}(t)) \notin X_{safe}$ will be safe for any initial condition $(\Delta x(0), \Delta\dot{x}(0), v_{lead}(0)) \in X_{safe}$. Under such control law, $(\Delta x(t), \Delta\dot{x}(t), v_{lead}(t))$ satisfies

$$-\Delta\dot{x}(t) < \max\left(-v_{lead}(t) + \sqrt{2a_{min}\Delta x(t) + v_{lead}^2(t) + v_{allow}^2(t)}, v_{allow}\right)\ . \tag{2.9}$$

The set of all $(\Delta x, \Delta\dot{x}, v_{lead})$ that satisfy (2.9) is denoted as $X_{bound} \subset X_{MS}$.

Theorem 2.1 implies the existence of a safety region, X_{safe}, in the $(\Delta x, \Delta\dot{x}, v_{lead})$ state space that is contained in X_{MS}. When the initial conditions for the relative motion of two platoons involved in a maneuver are inside this safety region an unsafe impact will not occur at any time if a control strategy is adopted such that whenever the state of the maneuver goes across the boundary ∂X_{safe} of X_{safe}, maximum braking is applied. This control strategy guarantees that the state of the maneuver will remain inside X_{bound}, a subset of X_{MS}, for all times $t \geq 0$. ∂X_{bound}, the boundary of X_{bound}, is the absolute safety boundary: for any initial state outside X_{bound} an unsafe impact in the sense of Definition 2.1 could occur if the lead platoon applies and holds maximum braking even if the trail platoon is braking at maximum capability. The schematic relations among these sets for a constant v_{lead} is illustrated in Fig. 2.2.

Eq. (2.8) implies that, when the relative distance Δx is initially large, the relative velocity can be greater that v_{allow}. However, if this relative distance is reduced, the relative velocity has to decrease to the point in which $-\Delta\dot{x}$ satisfies the second expression in Eq. (2.8). If the initial state $(\Delta x(0), \Delta\dot{x}(0), v_{lead}(0)) \in X_{MS} - X_{safe}$ and the lead vehicle applies full braking, then the trajectory described by the dynamics in Eqs (2.4)-(2.6) will necessarily produce an unsafe impact, even when the trail vehicle applies full braking. This constraint, that limits the maximum relative velocity depending both on v_{lead} and Δx, reduces the choices of initial states within X_{MS} and implies that $X_{safe} \subset X_{MS}$.

2.2 Properties of the safety region

The safety region suggested by Theorem 2.1 is dynamic in the sense that it depends on both lead and trail platoon's velocity and the relative distance between them. The 3-dimensional

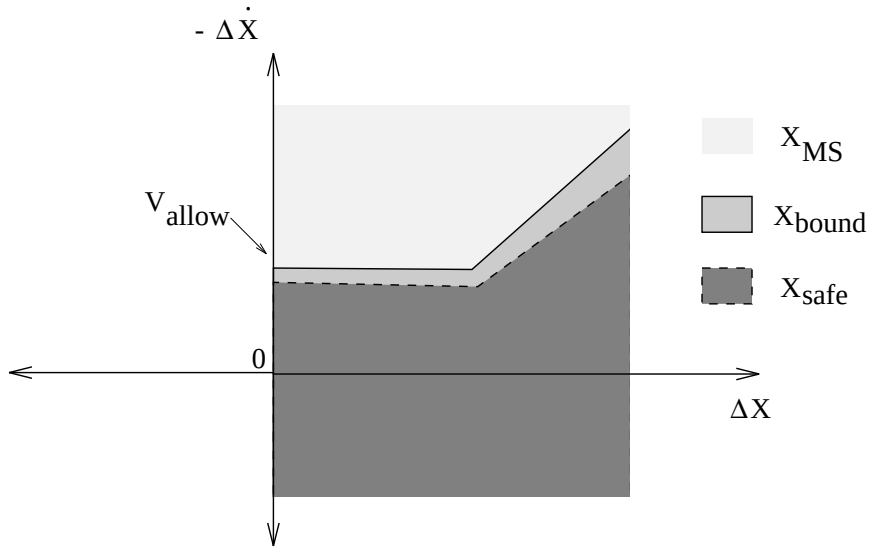

Figure 2.2: Relationship between X_{MS}, X_{bound} and X_{safe}.

mesh plot in Fig. 2.3 shows the boundary of this region in the $(\Delta x, \Delta\dot{x}, v_{lead})$ state space. The scales for the relative distance and the lead platoon velocity axes are chosen based on 60 m of radar sensing range and on a maximum traveling velocity on the highway of 40 m/s. The safety boundary is expressed in terms of the negative of the relative velocity of the two platoons, that is $-\Delta\dot{x} = \dot{x}_{trail} - \dot{x}_{lead}$.

If the lead platoon is running at a constant velocity, the safety boundary can be characterized by the 2-dimensional safety curve on the cross-sectional plane where v_{lead} equals the cruising speed. The safety curve is generally of the shape as the one shown in Fig. 2.2. The steep portion of the curve corresponds to the case where two platoons are far apart, the lead platoon suddenly applies full brakes and come to a complete stop before the trail platoon collide into it with a velocity no larger than the maximum allowable relative impact velocity, v_{allow}. The flat portion, on the other hand, stands for the case in which an impact occurs when both platoons are still in motion. It should be noted that as the lead platoon velocity decreases, the corresponding safety curve in the state space moves toward the relative distance axis in Fig. 2.3. For $v_{lead} = 0$, the horizontal portion does not exist. Fig. 2.4 shows the safety boundaries at different lead platoon velocities.

When the lead platoon is decelerating, the safety boundary will be a curve lying on the surface of Fig. 2.3. Fig. 2.5 shows the projections of a resulting safety curve on the $-\Delta\dot{x}$ vs. Δx and v_{lead} vs. Δx planes for the case where the spacing is 60 m, both platoons have an initial velocity of 15 m/s, the lead platoon brakes at a constant rate of $-2m/s^2$ and the trail platoons keeps constant velocity. The allowable relative impact velocity is $v_{allow} = 3m/s$.

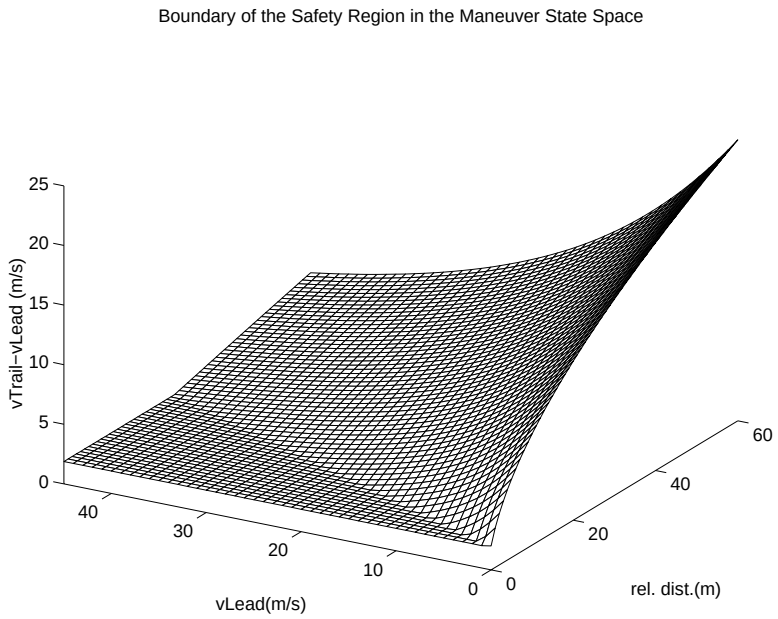

Figure 2.3: Boundary of the safety region in the $(\Delta x, \Delta \dot{x}, v_{lead})$ state space.

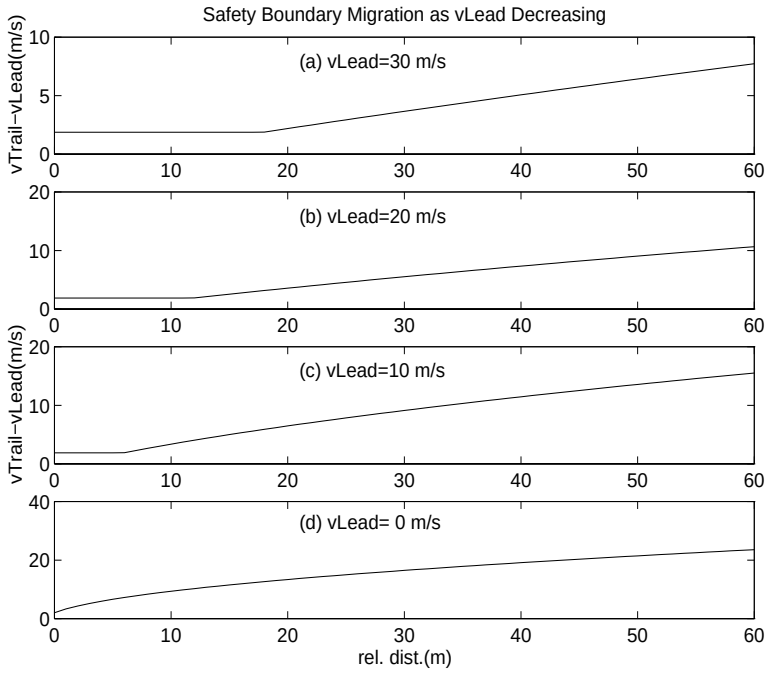

Figure 2.4: Safety boundary for different v_{lead}.

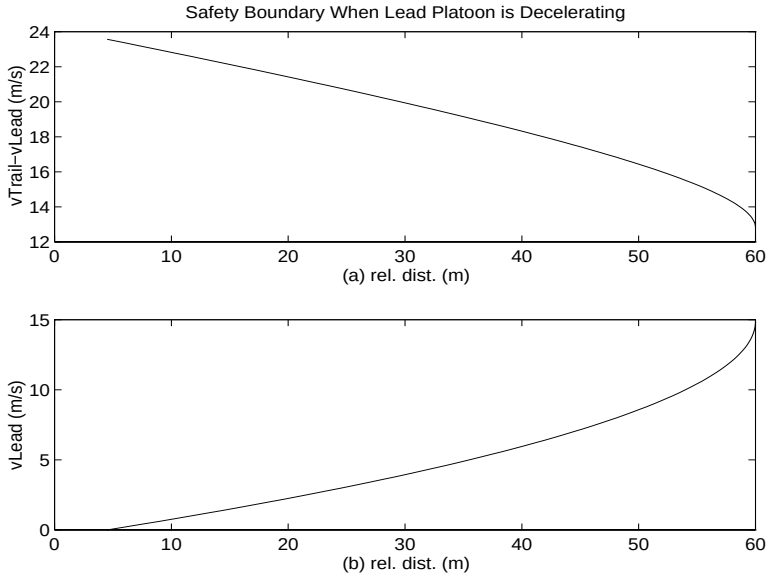

Figure 2.5: Projections of the safety boundary on the $-\Delta\dot{x}$ vs. Δx plane and on the v_{lead} vs. Δx plane. The lead platoon decelerates at $-2\,m/s^2$ and the trail platoon keeps a constant speed of 15 m/s.

Chapter 3

Trajectory Design

3.1 Maneuver trajectory on the $-\Delta\dot{x}$ vs. Δx plane

A safe maneuver trajectory should keep the maneuver state inside the safety region while trying to optimize the time for completion and the passenger comfort during the ride. Trajectories are designed based on a compromise between these requirements and physical capability constraints.

Assume that a desired velocity for the trail platoon in a maneuver has been specified as a function of the other states, i.e.,

$$\dot{x}_{trail} = v_{lead} + f(\Delta x, v_{lead})\,.$$

The acceleration, $\ddot{x}_{trail}$ and the jerk j_{trail} for the trail platoon that moves along this curve are:

$$\begin{aligned}
\ddot{x}_{trail} &= \ddot{x}_{lead} + \frac{\partial f}{\partial \Delta x}\frac{d\Delta x}{dt} + \frac{\partial f}{\partial v_{lead}}\frac{dv_{lead}}{dt} \\
&= \ddot{x}_{lead} + (v_{lead} - \dot{x}_{trail})\frac{\partial f}{\partial \Delta x} + \frac{\partial f}{\partial v_{lead}}\,\ddot{x}_{lead} \\
&= (1 + \frac{\partial f}{\partial v_{lead}})\ddot{x}_{lead} - f\frac{\partial f}{\partial \Delta x}\,, \qquad (3.1)
\end{aligned}$$

$$\begin{aligned}
j_{trail} &= \frac{d\ddot{x}_{trail}}{dt} \\
&= \frac{\partial \ddot{x}_{trail}}{\partial \Delta x}\frac{d\Delta x}{dt} + \frac{\partial \ddot{x}_{trail}}{\partial v_{lead}}\frac{dv_{lead}}{dt} + \frac{\partial \ddot{x}_{trail}}{\partial \ddot{x}_{lead}}\frac{d\ddot{x}_{lead}}{dt} \\
&= -f\frac{\partial \ddot{x}_{trail}}{\partial \Delta x} + \frac{\partial \ddot{x}_{trail}}{\partial v_{lead}}\ddot{x}_{lead} + \frac{\partial \ddot{x}_{trail}}{\partial \ddot{x}_{lead}}\dddot{x}_{lead}\,. \qquad (3.2)
\end{aligned}$$

Since $\ddot{x}_{lead}$ doesn't depend on Δx and v_{lead}, $\frac{\partial \ddot{x}_{lead}}{\partial \Delta x} = 0$ and $\frac{\partial \ddot{x}_{lead}}{\partial v_{lead}} = 0$, therefore after substituting Eq. (3.1) into Eq. (3.2) we obtain

$$\begin{aligned}
j_{trail} &= f\left[(\frac{\partial f}{\partial \Delta x})^2 + f\,\frac{\partial^2 f}{\partial \Delta x^2}\right] - \left[\frac{\partial f}{\partial v_{lead}}\frac{\partial f}{\partial \Delta x} + 2f\frac{\partial^2 f}{\partial \Delta x \partial v_{lead}}\right]\ddot{x}_{lead} \qquad (3.3) \\
&\quad + \frac{\partial^2 f}{\partial v_{lead}}\ddot{x}_{lead}^2 + (1 + \frac{\partial f}{\partial v_{lead}})\dddot{x}_{lead}\,.
\end{aligned}$$

Eqs. (3.1) and (3.3) indicate that if during a maneuver the lead platoon undergoes a velocity change, i.e. $\ddot{x}_{lead} \neq 0$, it would significantly affect the jerk and acceleration of the trail platoon as it moves along the desired trajectory in the state space.

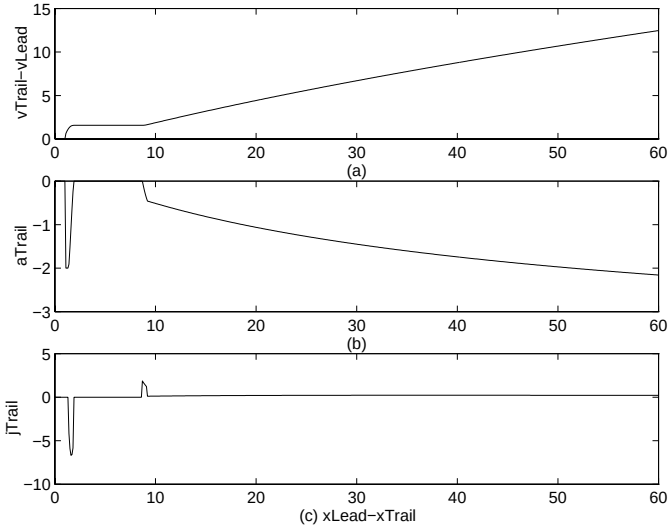

Figure 3.1: a_{trail} and j_{trail} needed for the join trajectory design in (Li et al., 1997). v_{lead} has a constant value of $15\,m/s$.

Fig. 3.1 gives an example of the acceleration and jerk requirements for the join maneuver trajectory proposed in (Li et al., 1997) for the normal of operation. In this case, the lead platoon maintains a constant velocity of $15\,m/s$. The first term of Eq. (3.1) and the last three terms of Eq. (3.2) vanish because $\ddot{x}_{lead} = 0$ and $\dddot{x}_{lead} = 0$ for a constant v_{lead}. When the transition region for splining is small, the proposed cubic spline in (Li et al., 1997) successfully smooths the transition of the trajectory from the flat portion to the deceleration curve, although it does not confine the jerk within the comfort constraints that are set to be $\pm 2.5 m/s^3$ (Aklar et al., 1979; Chiu et al., 1977; Hitchcock, 1994). This leads to a saturation in jerk in the controller in (Li et al., 1997). In the following section the choice of this transition region for the splining is determined so as to avoid this saturation.

3.2 New trajectory design for gap-closing maneuvers

As discussed in (Carbaugh, 1996; Li et al., 1997), there are several improvements that can be made to the maneuver trajectories in (Li et al., 1997), such as attaining zero acceleration at the end of the maneuvers and preventing the existence of low speed collisions, when the lead platoon applies and holds maximum braking. In order to minimize the time in which the maneuver is executed on the automated lanes, in (Frankel et al., 1994; Li et al., 1997) it is proposed to use the *follower law* to take care of the discrepancies existing between the actual and desired velocities and accelerations at the end of the maneuvers. A collision with a relative impact velocity lower than a safe limit is considered acceptable during an emergency. Thus, a reasonable performance can be reached for the automated lane maneuvers with the

current design.

However, during an entry, where all vehicles operate as "free agents", queuing in front of a stop light and moving towards another vehicle which is continuously changing its acceleration becomes the normal behavior. When this is the case, the existence of even low relative velocity collisions is undesirable. Moreover, a zero-acceleration ending condition is also necessary to form a queue without the need to switch to another control law.

The modifications proposed in this section are meant to eliminate the possibility of low speed collisions and to improve the end condition on acceleration in the current design. The saturation in jerk is also taken into consideration in the designing phase. These improvements induce additional completion time as their price. For the *stoplight* maneuver this trade-off between lower risk of collision and extra completion time is very acceptable.

3.2.1 Safety curve

Let's consider any control law for a maneuver whose purpose is to decrease the initial distance between two platoons in such a way that the maneuver is ended with zero relative velocity between the platoons. In order to maintain safety, the actual trajectory of the state $(\Delta x(t), \Delta\dot{x}(t), v_{lead}(t))$ should always be inside of the safety boundary X_{safe}. When two platoons are far enough from each other, we proposed to track the following curve

$$v_{safe1} = -(a_{max} + a_{min})d + \sqrt{2a_{min}\Delta x + v_{lead}^2 + a_{min}(a_{max} + a_{min})d^2}\,. \tag{3.4}$$

which is obtained by setting the maximum allowable relative impact velocity $v_{allow} = 0$ in the first expression of Eq. (2.8). Thus, in a maneuver perfectly tracking this desired trajectory collisions will not happen even if the lead platoon applies full braking. However, when platoons are close to each other and the braking capabilities in both are equal, not allowing any risk of collision will cause the maneuver to require an infinity amount of time to finish. The safety boundary from the second expression in Eq. (2.8),

$$v_{safe2} = v_{lead} - (a_{max} + a_{min})d + v_{allow}\,, \tag{3.5}$$

is then preserved for this portion of the desired curve. The expression for the modified desired velocity curve under the safety consideration for a given v_{lead} and Δx is

$$v_{safe}(\Delta x, v_{lead}) = \max(v_{safe1}, v_{safe2}) \tag{3.6}$$

The intersection of v_{safe1} and v_{safe2} occurs at

$$\Delta x_{Intxn1} = \frac{2v_{allow}v_{lead} + v_{allow}^2 - a_{min}(a_{max} + a_{min})d^2}{2a_{mim}}\,. \tag{3.7}$$

3.2.2 Finishing curve

In order to finish a *join* or *stoplight* maneuver it is necessary to bring the relative velocity of the two platoons to zero when the spacing reaches the designated distance. Using a quadratic minimum time curve with constant acceleration $-a_{com}$ for the final part of the maneuver

will lead to an oscillation around the desired final state because the final acceleration is not zero at the end of the maneuver. In (Li et al., 1997), it was assumed that the *join* maneuver control law is followed by the *follower* maneuver control law and that this control law would try to regulate around the final state. In this report we propose to use a cubic spline at the end of the trajectory that will lead to a zero acceleration at the target state. This cubic spline is of form

$$v_{decel1} = v_{lead} + a(\Delta x - \Delta x_d)^3 + b(\Delta x - \Delta x_d)^2 + c(\Delta x - \Delta x_d) + d\,. \tag{3.8}$$

The boundary conditions are

$$\begin{aligned} f(\Delta x_d) &= 0\,, \\ f'(\Delta x_d) &= 0\,, \\ f(\Delta x_d + \Delta x_{cubic}) &= \Delta v_{safe2}\,, \\ f'(\Delta x_d + \Delta x_{cubic}) &= 0\,. \end{aligned}$$

where

$f' = \frac{\partial f}{\partial \Delta x}$,
$\Delta\ x_{cubic}$ is the length of the cubic spline,
Δx_d is the desired final spacing,
$\Delta v_{safe2} = v_{safe2} - v_{lead} = -(a_{max} + a_{min})d + v_{allow}\,.$

The parameters a, b, c and d of the cubic spline, obtained by solving Eq. (3.8) with these boundary conditions, are

$$\begin{bmatrix} a \\ b \end{bmatrix} = -\frac{1}{\Delta x_{cubic}^4} \begin{bmatrix} 2\Delta x_{cubic} \\ -3\Delta x_{cubic}^2 \end{bmatrix} \Delta v_{safe2}\,, \tag{3.9}$$

$$\begin{bmatrix} c \\ d \end{bmatrix} = \begin{bmatrix} 0 \\ 0 \end{bmatrix}\,. \tag{3.10}$$

The derivation is detailed in Appendix A.1.

If the maximum acceleration of the trail platoon is not to exceed its maximum comfort level, and additional constraint must be imposed. This constraint, derived also in Appendix A.1, establishes a lower bound in the total length of the cubic spline, Δx_{cubic} and is given by

$$\Delta x_{cubic} \geq 0.9902\,\frac{\Delta v_{safe2}^2}{a_{com}}\,. \tag{3.11}$$

As long as Δx_{cubic} is chosen according to Eq. (3.11), the trail platoon acceleration at the target state will be zero and the magnitude of the maximum braking on this trajectory is guaranteed not to exceed the comfort level, a_{com}, under normal operation.

Notice, however, that this constraint in the length of the cubic spline, Δx_{cubic} is not sufficient to also guarantee that the magnitude of the jerk required on the spline will not exceed the comfort limit ($j_{com} = \pm 2.5\,m/s^3$ in (Frankel et al., 1994; Li et al., 1997)). To illustrate this consider Fig. 3.2 that shows, for the system capability settings in (Li

et al., 1997), the required acceleration and jerk for the finishing spline when $\Delta x_{cubic} = 0.9902\Delta v_{safe2}^2/a_{com}$. The extremum of the acceleration required on this trajectory is confined not to be larger than $-a_{com} = -2\,m/s^2$ as expected. However, the required jerk at the beginning of the cubic finishing curve is $-15.3244\,m/s^3$ which is larger than the comfort level. By selecting a large enough Δx_{cubic}, it is possible to have a finishing spline which satisfies both the jerk and acceleration comfort constraints. Fig. 3.3 shows such a choice of length, where $\Delta x_{cubic} = 3.0614\,m$.

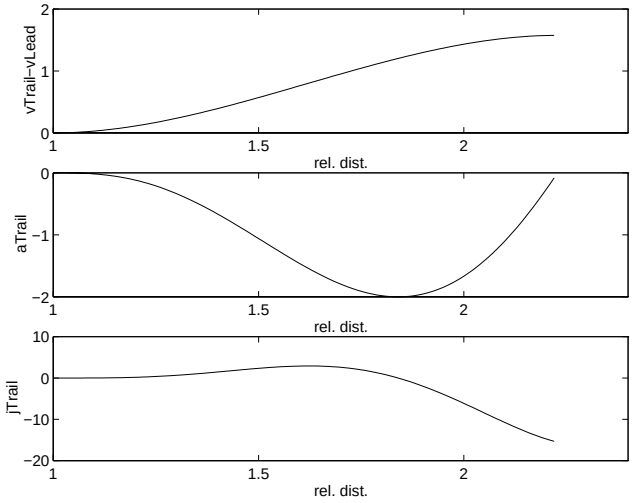

Figure 3.2: a_{trail} and j_{trail} needed for the new finishing spline. $\Delta x_{cubic} = 1.2282$ and the desired final spacing is $1\,m$.

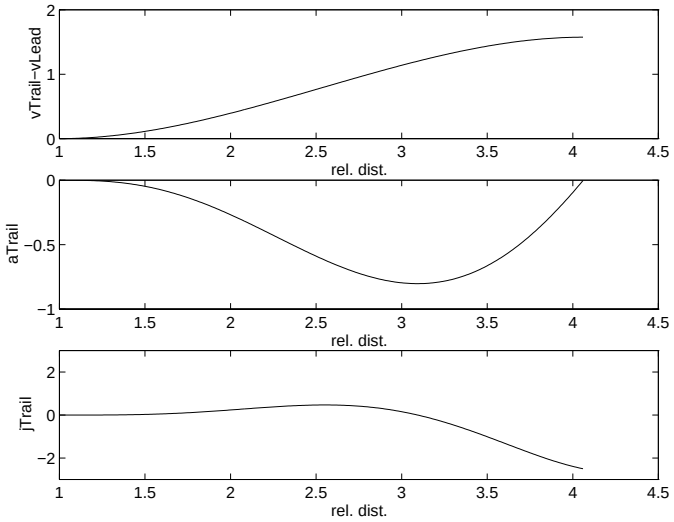

Figure 3.3: a_{trail} and j_{trail} needed for the new finishing spline. $\Delta x_{cubic} = 3.0614$ and the desired final spacing is $1\,m$.

A deceleration curve given by Eq. (3.8) is appropriate when the safety boundary possesses a shape similar to those in Fig. 2.4 (a)-(c). When the velocity of the lead platoon

is sufficiently low, the curve given by Eq. (3.8) is entirely below the one in Eq. (3.6) and therefore there are not valid boundary conditions to solve for the spline curve parameters. To solve this problem, another deceleration curve which consists of a constant deceleration curve together with the cubic spline described above is used. This curve is

$$v_{decel2} = \begin{cases} v_{lead} + \sqrt{\Delta v_{ext}^2 + 2a_{com}(\Delta x - \Delta x_{ext})}\,; & \Delta x \geq \Delta x_{ext}\,, \\ v_{lead} + a(\Delta x - \Delta x_d)^3 + b(\Delta x - \Delta x_d)^2\,; & \Delta x \leq \Delta x_{ext}\,. \end{cases} \tag{3.12}$$

where Δx_{ext} is the spacing at which the acceleration of the trail platoon for the cubic spline given by Eq. (3.8) has an extreme value. Δv_{ext} is the corresponding relative velocity. They can be obtained from the following equations

$$\begin{aligned} \Delta x_{ext} &= \Delta x_d + \beta\frac{a}{b}\,, \\ \Delta v_{ext} &= (\beta^2 - \beta^3)\frac{b^3}{a^2}\,. \end{aligned} \tag{3.13}$$

where $\beta = -0.4558$, a and b are given by Eq. (3.9). The derivation of Eq. (3.13) is detailed in Appendix A.1.

Thus, the desired velocity profile which satisfies the requirements of safety, the minimum completion time, and the zero final acceleration is given by

$$v_d(\Delta x, v_{lead}) = \begin{cases} \min(v_{safe}, v_{decel1}, v_{max})\,; & \Delta x_{Intxn1} \geq \Delta x_d + \Delta x_{cubic}\,, \\ \min(v_{safe}, v_{decel2}, v_{max})\,; & \Delta x_{Intxn1} < \Delta x_d + \Delta x_{cubic}\,. \end{cases} \tag{3.14}$$

where v_{max} is the maximum velocity for platoons to travel in the highway.

The deceleration curves, v_{decel1} and v_{decel2}, are for the case in which the lead platoon maintains a constant velocity. If the lead platoon has an acceleration, Eq. (3.11) and (3.12) have to be modified by replacing a_{com} with an acceleration a_{hybrid} which can compensate the effect induced by the lead platoon acceleration, $\ddot{x}_{lead}$. The acceleration necessary to track a desired trajectory f is described in Eq. (3.1). The general expression for a trajectory which brings the current state to an arbitrary state with a constant acceleration, a_{hybrid}, is given by

$$f(\Delta x, v_{lead}) = \dot{x}_{trail} - \dot{x}_{lead} = \sqrt{\Delta v_{des}^2 + 2a_{hybrid}(\Delta x - \Delta x_{des})}\,, \tag{3.15}$$

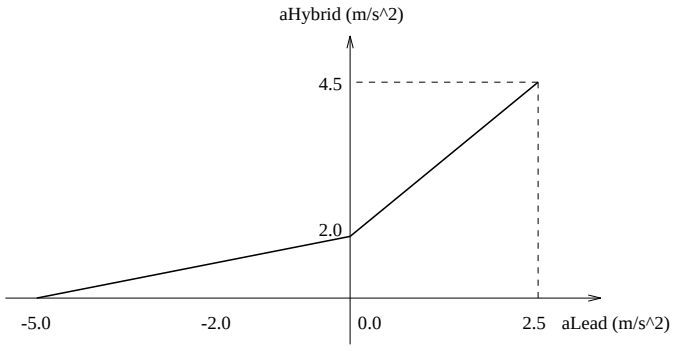

Figure 3.4: Hybrid acceleration a_{hybrid} vs. Lead platoon acceleration a_{lead}.

where Δv_{des} and Δx_{des} are relative velocity and relative spacing of the destination state. It should be noted that, in the presence of $\ddot{x}_{lead}$, the acceleration a_{hybrid} will not be the comfort acceleration of the trail platoon alone. It should be determined based on the accelerations of both platoons. Substituting Eq. (3.15) into (3.1) we obtain, as expected, that

$$a_{hybrid} = \ddot{x}_{lead} - \ddot{x}_{trail} \,. \tag{3.16}$$

In order to maintain a good compromise between safety and the passenger comfort, the following strategy is used in the presence of the lead platoon acceleration:

$$\begin{cases} \ddot{x}_{trail} = -a_{com} \,; & \ddot{x}_{lead} \geq 0 \,, \\ \ddot{x}_{trail} = -a_{com} + \frac{(a_{min} - a_{com})}{a_{min}} a_{lead} \,; & \ddot{x}_{lead} < 0 \,. \end{cases} \tag{3.17}$$

Fig. 3.4 shows the relationship between a_{lead} and the corresponding a_{hybrid}. Note that $\ddot{x}_{trail}$ and $\ddot{x}_{lead}$ are bounded in the range of $[-a_{min}, a_{max}]$ and that a_{hybrid} is never negative. A negative value in a_{hybrid} implies a harder braking in the lead platoon than in the trail platoon. Collision becomes inevitable in this case as the assumption on the same braking capabilities is violated.

Chapter 4

Implementation of Maneuvers

4.1 Join maneuver

The desired trajectory designed in Chapter 3 is directly applicable to the *join* maneuver, whose goal is to bring the initial spacing $\Delta x(0)$ between two platoons to a desired intraplatoon spacing Δx_d in minimum time, ensuring safety during the process. At the end of the maneuver, the trail platoon should have zero relative velocity with respect to the lead platoon, i.e. $\dot{x}_{trail} - \dot{x}_{lead} = 0$. The desired trajectory for the generic controller is given by Eq. (3.14). Simulation results are shown in Chapter 5.

4.2 Stoplight maneuver

The purpose of the *stoplight* maneuver is to move vehicles in the entry lane of the automated highway. A typical configuration of an AHS entry is shown in Fig. 4.1. In the AHS entry/exit design in (Godbole et al., 1995), it is proposed that at the entrance a check station is used to signal the upcoming vehicle the distance to a stop light in front of which vehicles should stop and wait for the permission to merge into the highway traffic. If there is more than one vehicle, vehicles have to queue in the entry. As the queue advances, every vehicle in it will eventually reach the stop light. Once permission is granted, the vehicle accelerates, changes lane, and becomes part of the automated highway traffic. *Stoplight* is the longitudinal maneuver used to control the arrival of vehicles to the stop light.

The *stoplight* maneuver is implemented using the safe controller structure in (Li et al., 1997). The finite state machine in Fig. (4.2) is used to determine the object with respect to which the desired velocity is calculated, i.e., another vehicle or the stop light.

When a vehicle goes into a transition lane, the coordination layer initiates the *stoplight* maneuver by informing the vehicle the distance to the stop light from the check station. If there is no other vehicle in the sensing range of its on board longitudinal sensor, the controller will calculate the desired velocity trajectory solely with respect to the stop light (*State1*). However, since the sensing range of the on board sensor is limited and usually cannot cover the whole length of the entry, the velocity to travel in the entry should be bounded in such a way that a collision can always be avoided by using comfort braking. Thus, the desired

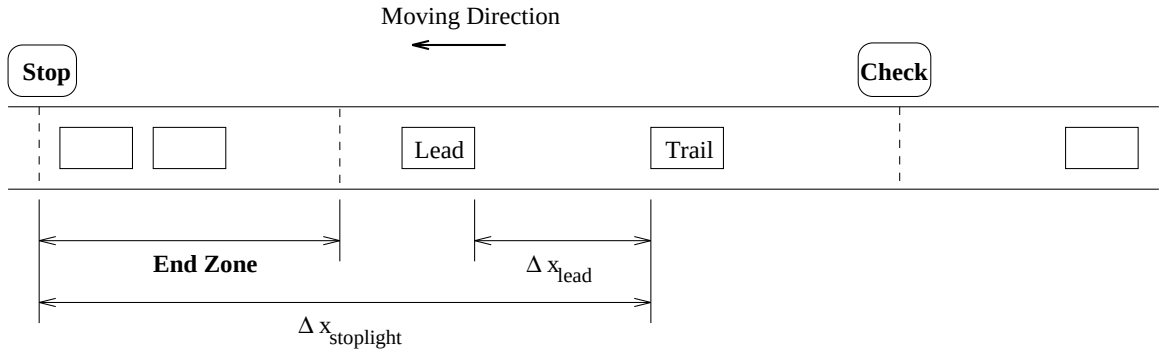

Figure 4.1: Configuration of an entry transition lane.

velocity with respect to the stop light is

$$v_d^{stoplight} = \min(v_{safe}(\Delta x_{stoplight}, 0),\ v_{decel1}(\Delta x_{stoplight}, 0),\ v_{max}^{trans})\,, \tag{4.1}$$

where $\Delta x_{stoplight}$ is the relative distance to the stoplight, v_{max}^{trans} is the maximum allowable velocity on the transition lane, v_{safe} and v_{decel1} are obtained from Eq. (3.6) and (3.8) respectively.

If there is a vehicle within the sensing range (*State2*), the entry vehicle has to queue and the state of this vehicle immediately in front has to be used to calculate the desired trajectory.

$$v_d^{lead} = v_d(\Delta x_{lead}, v_{lead})\,. \tag{4.2}$$

where the v_d is given by Eq. (3.14) with the v_{max} substituted by v_{max}^{trans}. Δx_{lead} and v_{lead} denote the relative distance and the lead vehicle velocity respectively.

To finish the *stoplight* maneuver smoothly when other vehicles are present in front and the stop light is within the *End zone* range, it is necessary to calculate the desired velocities with respect both the front vehicle and the stop light (*State 3*). The desired velocity curve

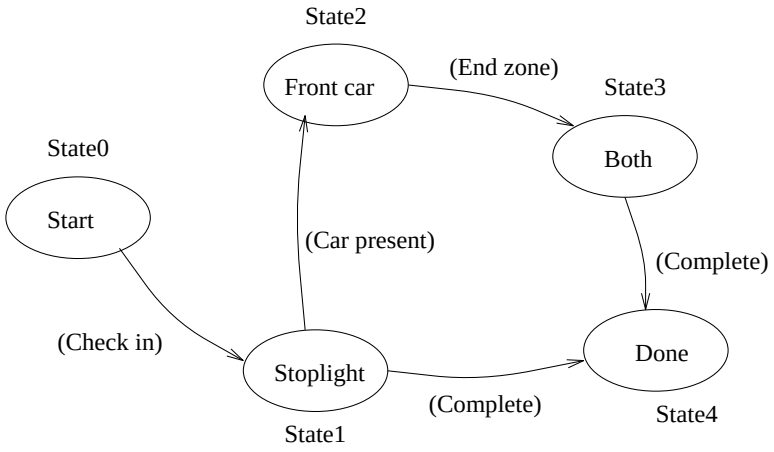

Figure 4.2: State machine for the *stoplight* maneuver.

is

$$v_d^{endzone} = \min(v_d^{stoplight}, v_d^{lead}) \,. \tag{4.3}$$

4.3 Frontdock maneuver

The *frontdock* maneuver (Fig. 4.3) was defined in (Lygeros et al., 1995) for the degraded modes of operation of the AHS architecture in (Varaiya and Shadlover, 1991). The goal of this maneuver is to decelerate a vehicle to close up the gap between itself and a faulty vehicle behind it. An the end of the *frontdock* maneuver, the vehicle that decelerates becomes a platoon leader and the faulty vehicle becomes the first follower of the new platoon. The *frontdock* maneuver can be interpreted as a "reverse" *join*.

The controller in (Li et al., 1997) is also used for this maneuver. The trajectory design philosophy in Chapter 3 is used. According to the safety analysis, in order to maintain safety in the sense of Definition 2.2, the velocity of the trail vehicle has to be greater than

$$\begin{aligned} \dot{x}_{trail}(t) \;\geq\; & \max(v_{faulty} + (a_{max} + a_{min})d + \Delta v_{buff} \\ & -\sqrt{v_{allow}^2 + 2(a_{max} - a_{faulty})\Delta x_{faulty}}, 0) \,, \end{aligned} \tag{4.4}$$

for a given faulty vehicle velocity v_{faulty} and a given relative distance, $\Delta x_{faulty} = x_{trail} - x_{faulty}$. Since the assumption on the fault tolerant AHS design in (Lindesy, 1996) states that once a *frontdock* maneuver is requested, the faulty vehicle itself will attempt to maintain its current velocity by executing a *constvel* (constant velocity) maneuver, the maximum acceleration for the faulty vehicle, a_{faulty}, will be constrained to a small value and this value will only occur under some extreme conditions, for instance, in the case of losing brakes on a steep slope. Δv_{buff} in the equation is a factor of safety.

The desired velocity for safety purposes is proposed by setting v_{allow} in Eq. (4.4) to zero to avoid collisions in this maneuver, that is

$$v_{safe}^{frontdock} = \max(v_{faulty} + (a_{max} + a_{min})d + \Delta v_{buff} - \sqrt{2(a_{max} - a_{faulty})\Delta x_{faulty}}, 0) \,. \tag{4.5}$$

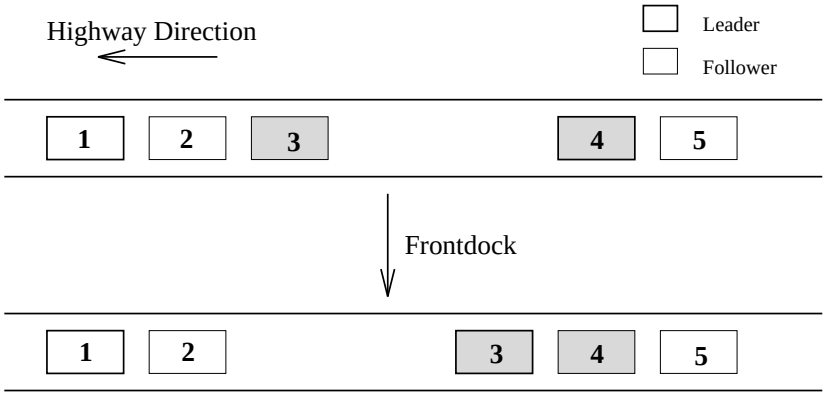

Figure 4.3: *Frontdock* maneuver.

To finish the maneuver in minimum time and zero acceleration, instead of a cubic spline curve, a quadratic spline is used:

$$v_{decel}^{frontdock} = a\Delta x_{faulty}^2 + b\Delta x_{faulty}^2 + c, \quad \Delta x_{faulty} \leq \Delta x_{spline}\,, \tag{4.6}$$

where

$$\begin{aligned} a &= -\frac{27(a_{max} - a_{faulty})^2}{64[(a_{max} + a_{min})d + \Delta v_{buff}]^3}\,, \\ b &= 0\,, \\ c &= v_{faulty}\,, \\ \Delta x_{spline} &= \frac{8[(a_{max} + a_{min})d + \Delta v_{buff}]^2}{9(a_{max} + a_{min})}\,. \end{aligned}$$

The complete derivation is detailed in Appendix A.2.

It should be noted that since the purpose of the *frontdock* control law is to bring the trail vehicle to be in contact with the faulty vehicle at the end of the maneuver, so that a subsequent maneuver can utilize the brakes of the trail vehicle to stop the faulty vehicle on the highway, the desired final spacing is zero.

The desired velocity profile for the trail platoon is given by

$$v_d = \begin{cases} v_{safe}^{frontdock}; & \Delta x_{faulty} > \Delta x_{spline}\,, \\ v_{decel}^{frontdock}; & \Delta x_{faulty} \leq \Delta x_{spline}\,. \end{cases} \tag{4.7}$$

In addition, a safety strategy is used that requires $\dot{x}_{trail}$ also to satisfy the following criterion:

$$\dot{x}_{trail}(t) \leq v_{safe}(\Delta x_{lead}, v_{lead})\,, \tag{4.8}$$

where $v_{safe}(\Delta x_{lead}, v_{lead})$ is the safety bound with respect to the vehicle in front of the trail car and is obtained from Eq. (3.6). Δx_{lead} and v_{lead} are the relative distance and lead vehicle velocity respectively.

Chapter 5

Simulation Results

Simulation results given in this chapter are from a simulation tool program developed in order to facilitate easy maneuver development and verification outside of the SmartPath environment. This program is capable of simulating not only maneuvers which involve two platoons but also those multiple platoon maneuvers such as *frontdock* and *stoplight*. The regulation layer control laws were implemented in SmartPath modules, tested in this testing environment, and ported to SmartPath for the full scale AHS simulation.

These simulations are conducted under the assumption that all vehicles on the AHS have the same capability in terms of acceleration, deceleration, delay, and so on. This may not be true on an actual system where the traffic is usually a mixture of different types of cars. The results of research regarding the effect of different capabilities in (Alvarez, 1996) can be incorporated to the results of this report.

The same set of system parameters used in (Li et al., 1997) is adopted and summarized below:

- $a_{com} = \pm 2\, m/s^2$.
- $a_{min} = 5\, m/s^2$.
- $a_{max} = 2.5\, m/s^2$.
- $j_{com} = \pm 2.5\, m/s^3$.
- $j_{max} = \pm 50\, m/s^3$.
- $v_{allow} = 3\, m/s$.

In addition, we use

- $d = 0.15\, sec$, which is determined from the jerk constraint.
- $a_{faulty} = 0.6\, m/s^2$.
- $\Delta x_d^{join} = \Delta x_d^{stoplight} = 3\, m$.

for the simulations presented in this chapter. Note that in a SmartPath simulation, the pick for the desired intra-vehicle spacings is decided dynamically by the upper layer controller and is not necessary to be the value we select here.

The gains for the control laws and their associated reduced-order state observers (see (Li et al., 1997) for the structure) are

$$\lambda_1 = 0.3,\ \lambda_2 = 15,\ \beta = 2,\ \gamma = 1.2,\ L_1 = 0.3,\ L_2 = 10\,.$$

5.1 Simulations for *join* maneuver

Fig. 5.1 shows results for a *join* using the new trajectory design with a initial spacing of $60\,m$. Both platoons start with a initial velocity of $25\,m/s$. During the maneuver, the lead platoon manages to maintain a constant velocity. The maneuver finished at $t = 25.33$ *sec* in comparison to 21.81 *sec* of the trajectory design in (Li et al., 1997). The relative velocity and zero acceleration are zero at the end of the maneuver. The 16.14% increase in the time for completion can have a significant impact on the AHS capacity under the normal operation.

Fig. 5.2 is for a *join* from the same distance of $60\,m$ although with a lower initial velocity of $5\,m/s$ for both platoons. The simulation shows that the trajectory has a perfect "lockup" at the end of the maneuver. The completion time for executing this maneuver is $12.77\,sec$ vs. $11.90\,sec$ of the current design, or 7.31% increase in time. This small increase suggests that the proposed trajectory design would be suitable for the *stoplight* maneuver in an entry.

In Fig. 5.3 a *join* is initiated from $60\,m$ of spacing with both platoons running at $25\,m/s$. Instead of keeping a constant velocity, the lead platoon brakes at its maximum braking capability, $-5\,m/s^2$, immediately after the maneuver starts. By joining defensively, the trail platoon reacts not only to the spacing and the lead platoon's velocity but also to lead platoon's acceleration. At some point during the process, these two platoons were actually braking with the same capability and the relative velocity was maintained until the lead platoon eventually came to a complete stop. Then, the trail platoon retrieved its acceleration and finished the maneuver. It is shown that by joining defensively and adopting the more conservative safety curve v_{safe1} of Eq. (3.4), it is possible to avoid a collision under severe situations if the distance is large enough.

Fig. 5.4 is a comparison where a collision is inevitable in the current trajectory design. The maneuver starts from $60\,m$ of initial spacing with $25\,m/s$ of initial velocities in both platoons. The lead platoon applies and holds maximum braking when $\Delta x = 50\,m$ at $t = 3.63\,sec$. Collision is avoided by using the new trajectory design.

Fig. 5.5 shows another example of *join* where two platoons have $60\,m$ of initial spacing and initial velocities of $25\ m/s$. The lead platoon suddenly applies full brakes when the spacing is $\Delta x = 13.68\,m$ and the trail platoon is tracking the v_{safe2} portion of the desired trajectory. Because of the deceleration curve's reaction to the deceleration of the lead platoon, the maneuver is finished without collisions even though the v_{safe2} is designed to be v_{allow} safe.

Fig. 5.6 shows the most extreme case where the lead platoon brakes and holds the maximum capability when the two platoons are very close to each other ($\Delta x = 5.8149\,m$), because of the effect of the delay, a collision occurs before the trail platoon can achieve its maximum braking. However, as expected, the relative impact is lower than the specified v_{allow}.

In order to finish the maneuver in finite time, it is unrealistic not to allow any collision to happen when braking capabilities are assumed equal for both platoons. A maximum allowable relative impact velocity v_{allow} is thus specified for the situation when two platoons are close to each other. The simulation results in Figs. 5.3 to 5.5 show that by adopting a deceleration curve which is dynamic not only to the relative spacing Δx and lead platoon

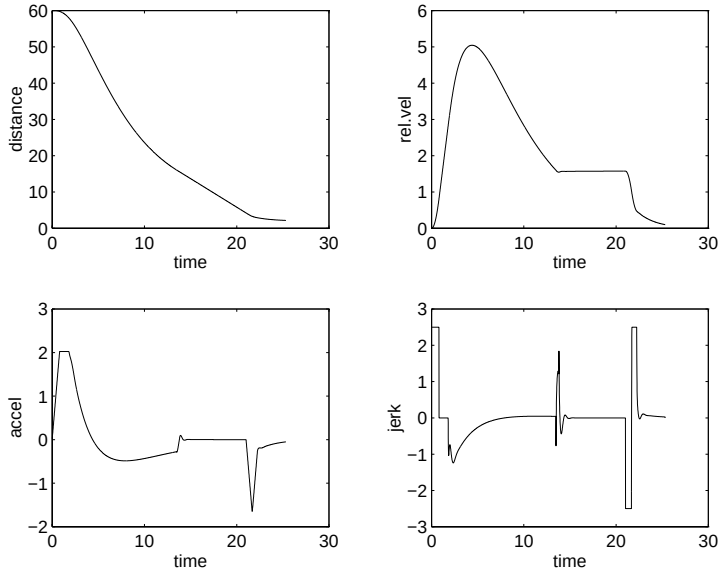

Figure 5.1: Simulation Results of the *join* maneuver from an initial spacing of 60 m. The lead platoon maintains a constant velocity of 25 m/s.

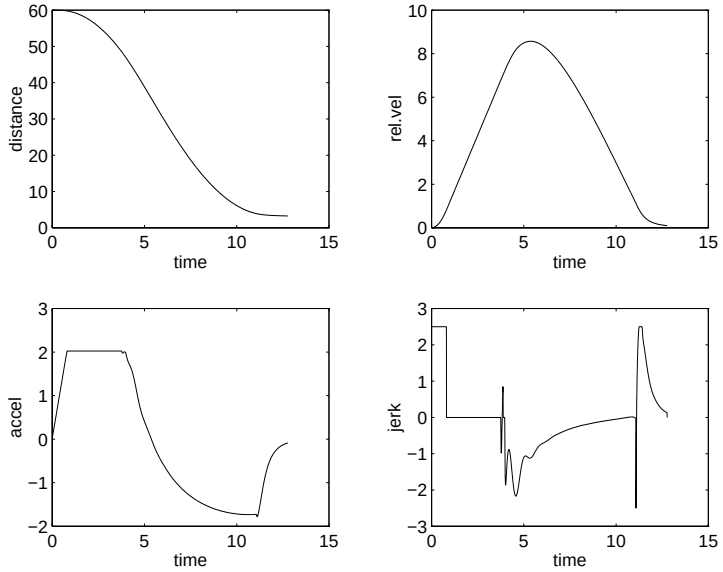

Figure 5.2: Simulation results of the *join* maneuver from an initial spacing of 60 m. The lead platoon maintains a constant velocity of 5 m/s.

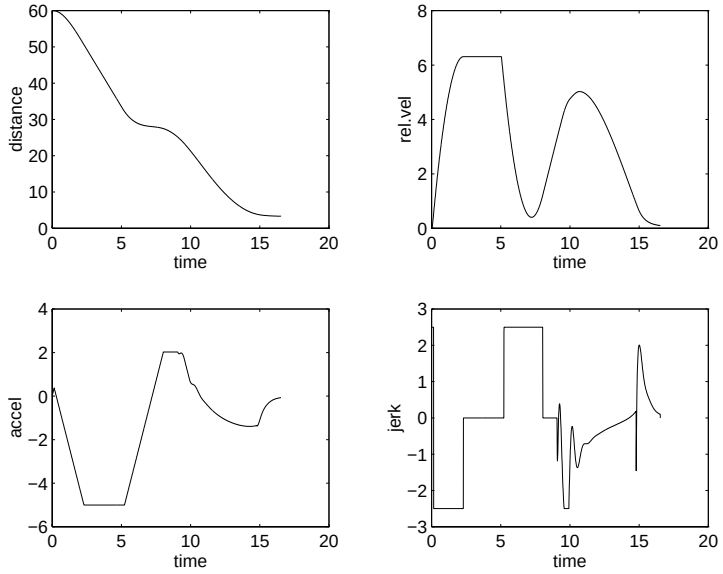

Figure 5.3: Simulation results of the *join* maneuver from an initial spacing of 60 m. The lead platoon applies maximum braking $-a_{min} = -5m/s^2$ when $\Delta x = 60\,m$.

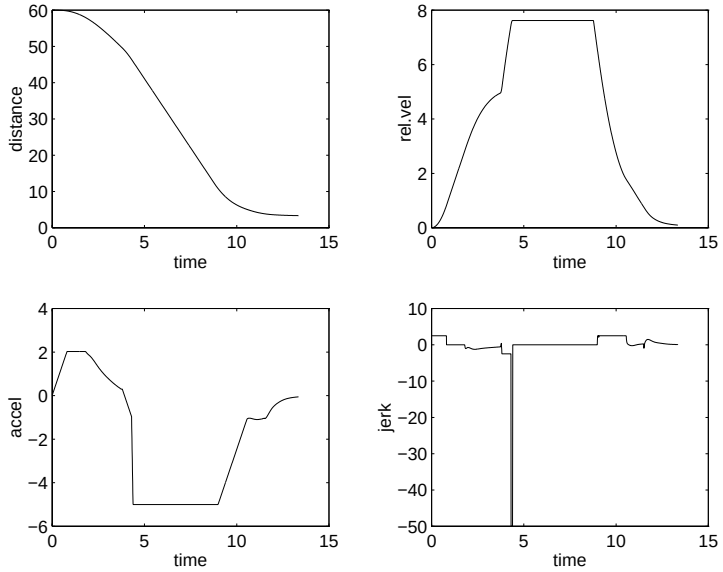

Figure 5.4: Simulation results of the *join* maneuver from an initial spacing of 60 m. The lead platoon applies maximum braking $-a_{min} = -5m/s^2$ when $\Delta x = 50\,m$.

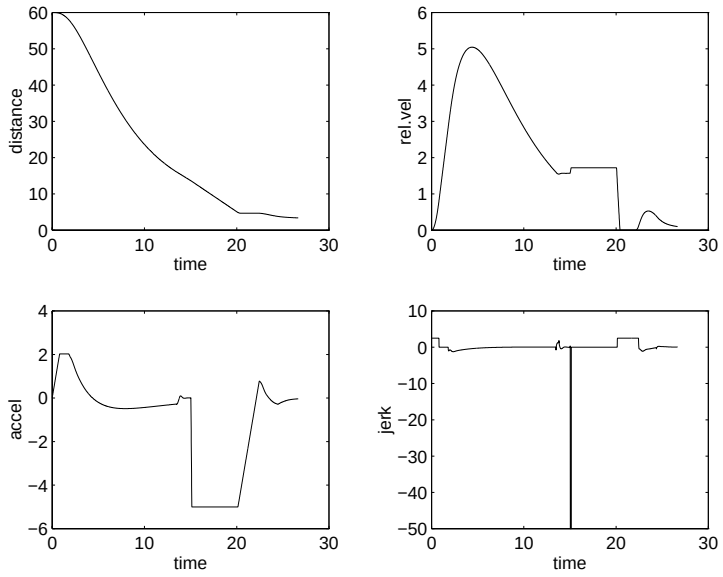

Figure 5.5: Simulation results of the *join* maneuver from an initial spacing of 60 m. The lead platoon applies maximum braking, $-a_{min} = -5\,m/s$ at $\Delta x = 13.68\,m$.

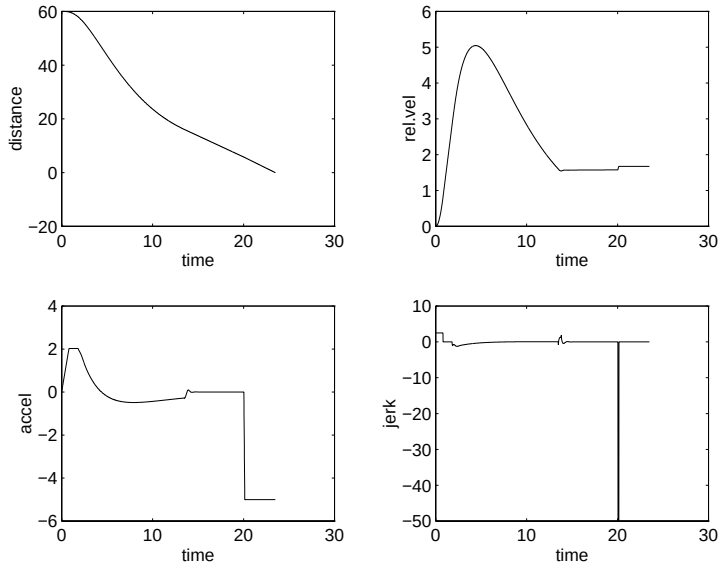

Figure 5.6: Simulation results of the *join* maneuver from an initial spacing of 60 m. The lead platoon applies maximum braking, $-a_{min} = -5\,m/s$ when $\Delta x = 5.814\,m$.

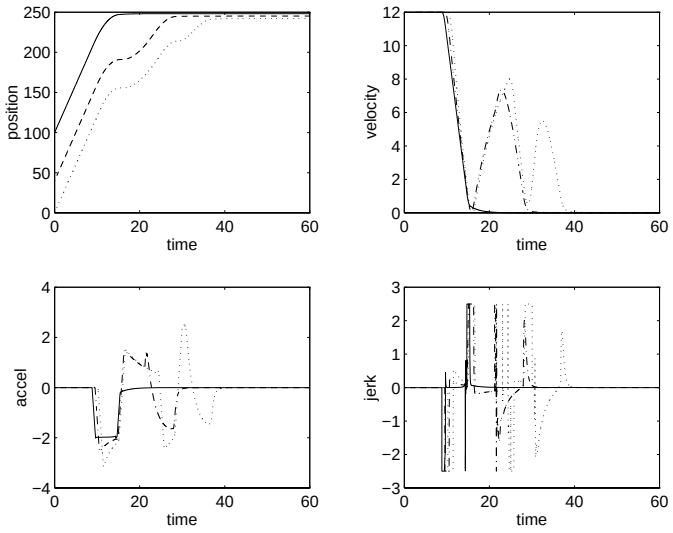

Figure 5.7: Simulation results of the *stoplight* maneuver. Initial configuration: three vehicles at 100 m, 40 m and 0 m from the check station.

velocity v_{lead} but also to lead platoon's acceleration it is possible to bring the maneuver state to the desired final state and minimize the possibility of collisions under severe disturbances. The only collision in the simulations occurred when the two platoons were very close, as illustrated in Fig. 5.6 for $\Delta x = 5.814\,m$, and the lead platoon suddenly applied and held maximum braking. Because of the effect of the delay, an collision becomes inevitable. However, this impact is still considered to be safe in the sense of Definition 2.2.

5.2 Simulations for *stoplight* maneuver

Fig. 5.7 shows the case where the stop light is located $250\,m$ away from the check station. The initial layout for vehicles in this entrance is that three *free agents* executing *stoplight* maneuver are positioned at $100\,m$, $40\,m$ and $0\,m$ initially, whereas in Fig. 5.8 they are at $40\,m$, $20\,m$ and $0\,m$, and in Fig. 5.9 at $140\,m$, $70\,m$ and $0\,m$, respectively. These two last distributions of vehicles intent to illustrate the behavior of densely distributed and loosely distributed vehicles in the entrance. The solid line represents the leading vehicle, the dash-dot line stands for the second one, and the last vehicle is shown by the dotted line in these simulation results. Desired final intra-vehicle spacing is $3\,m$ in all these simulations.

It is shown that in all three cases, vehicles manage to reach the stop light without slamming on their brakes. No collision occurs even in the presence of continually varied accelerations of the vehicles in front. Also note that the high control activity in terms of jerk for vehicles which are not the leading car are the result of the defensive control strategy to the varied accelerations of the front cars.

This conservative acceleration and defensive reaction to the acceleration variation of the lead platoon are the two major features in the trajectory design. They may not seem obviously advantageous for the class of normal mode maneuvers in the automated lanes since in targets platoons are normally traveling at constant velocity. However, these acceleration

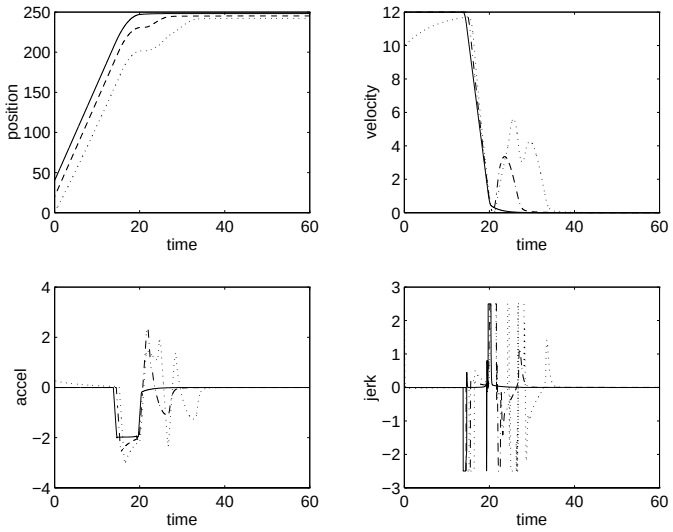

Figure 5.8: Simulation results of the *stoplight* maneuver. Initial configuration: three vehicles at 40 m, 20 m and 0 m from the check station.

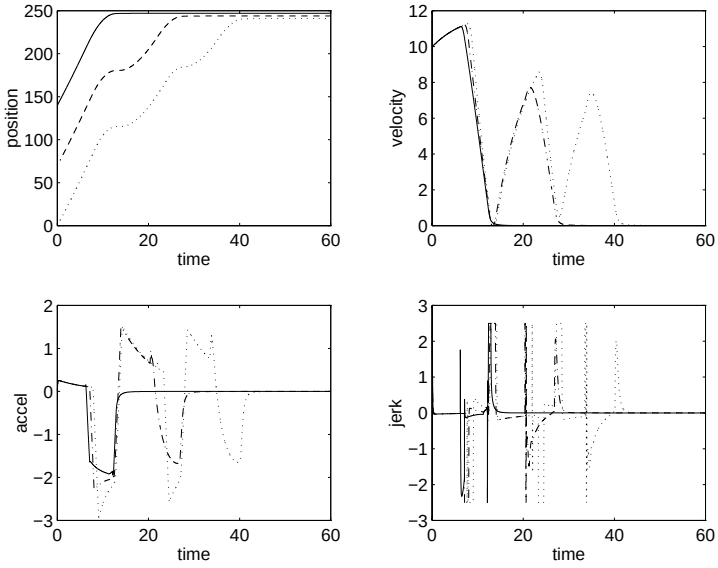

Figure 5.9: Simulation results of the *stoplight* maneuver. Initial configuration: three vehicles at 140 m, 70 m and 0 m from the check station.

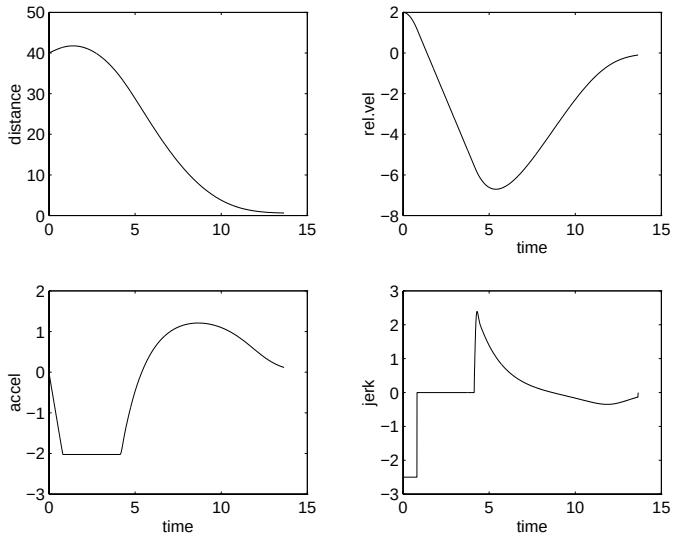

A *Frontdock* maneuver is requested by a faulty vehicle at time $t = 0$ with an initial spacing of 40 m. The faulty vehicle maintains it's initial velocity of 23 m/s by executing the *constvel* control law. The trail vehicle has an initial velocity of 25 m/s. Relative distance is given by $\Delta x = x_{trail} - x_{faulty}$ and relative velocity is by $\Delta v = \dot{x}_{trail} - \dot{x}_{faulty}$.

Figure 5.10: Simulation results of the *frontdock* maneuver with new trajectory.

patterns become significantly advantageous in the *stoplight* maneuver of the transition lane. Since the behavior of a vehicle in a transition lane is a complex dynamical consequence of the vehicles in front, joining to a vehicle continually accelerating or decelerating is essential in order to accomplish the task of moving vehicles sequentially to the stop light.

5.3 Simulations for *frontdock* maneuver

Simulation results are also provided for the *frontdock* degraded mode maneuver. Instead of joining to a vehicle in front, the *frontdock* maneuver requires the vehicle who executes it to decelerate and eventually to make contact with the faulty vehicle in the back. By utilizing the trajectory design in Chapter 4, a docking vehicle is then able to have a "soft" join with respect to the faulty vehicle at the end of the maneuver. However, the lengthened time using this trajectory may impact the speed to recover from the fault on the highway. This, in turn, affects the highway throughput.

Fig. 5.10 shows the execution of a *frontdock* maneuver with the a faulty vehicle that is maintaining its velocity by executing a *constvel* (constant velocity) maneuver. The trail vehicle, which is the one that docks into the faulty car, decelerates and tracks the trajectory detailed in Section 4.3. As expected, the contact at the end of the maneuver is made "soft" with the cost of completion time increased from 11.02 *sec* of the current design to 13.62 *sec*. Note that the both the final acceleration and jerk are zero. Acceleration and jerk used are within the comfort bounds throughout the maneuver. Fig. 5.11 is a comparison where the current trajectory design is used.

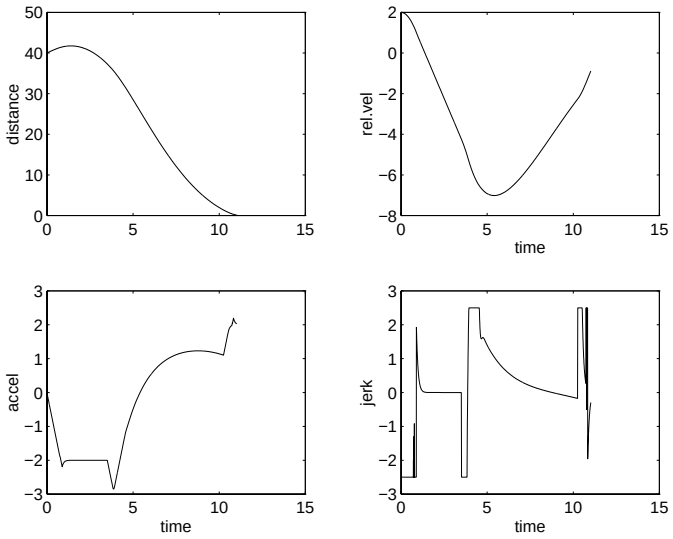

A *Frontdock* maneuver is requested by a faulty vehicle at time $t = 0$ with an initial spacing of 40 m. The faulty vehicle maintains it's initial velocity of 23 m/s by executing the *constvel* control law. The trail vehicle has an initial velocity of 25 m/s. Relative distance is given by $\Delta x = x_{trail} - x_{faulty}$ and relative velocity is by $\Delta v = \dot{x}_{trail} - \dot{x}_{faulty}$

Figure 5.11: Simulation Results of the *frontdock* maneuver with the previous trajectory.

One should notice that the simulation presented here is under the assumption that only a single fault is dealt with at a time. In the case when there is a double fault, and the lead platoon is forced to apply full brakes while the trail platoon is executing the *frontdock*, this maneuver is intrinsically unsafe. The safety of this maneuver under this condition cannot be guaranteed by the regulation layer alone.

Chapter 6

Conclusion

In this report we presented a modification to the safe trajectory proposed in (Li et al., 1997) for the regulation layer maneuvers. This new design relies in a more conservative behavior for the trail platoon. Explicit constraints for the splining between the regions of the safety trajectory are also imposed in order to guarantee comfort under normal conditions. The new trajectory design can avoid even low speed collisions for most of the cases. Only disturbances that occur when platoons are close to each other may produce collisions, altough the collisions have always a relative velocity below the given safety threshold. The price for the higher degree of safety is tolled in extra completion time.

The new design is applied to *join* maneuver in the normal mode of operation, to the *frontdock* maneuver in degraded mode and also to the *stoplight* maneuver in the transition lane. In order to achieve zero-acceleration at the end of this maneuver, a finishing curve which is dynamic to the acceleration of the object platoon is proposed. Control laws for *stoplight*, *join* and *frontdock* with the proposed trajectories are implemented. Simulation results are presented and performance analyses are made.

For a vehicle in an entry transition lane executing the *stoplight* maneuver, the extra time for completion is small. This increase is acceptable because the normal behavior for an entry vehicle will be that of joining a vehicle in front which continually varies its acceleration; frequent stopping is also common in this case. For the *join* maneuver in the normal mode of operation the increase of time for completion is relatively larger and therefore will have a greater impact on the highway throughput. Whether or not to adopt these new trajectories will depend on a good engineering decision.

These trajectories are designed under the assumption that all vehicles have identical braking and accelerating capabilities. In the case where vehicles' capabilities are different, a further modification is possible following the results in (Alvarez, 1996). Even though the successful results under extensive simulations indicate that the designed *stoplight* maneuver with this trajectory is likely to perform well in the dynamically hard transition lane, a more extensive analysis for a string of vehicles running independently in the transition lane is still needed.

Bibliography

Aklar, S. J., Bevans, J. P., and Stein, G. (1979). 'Safe-approach' vehicle follower control. *IEEE Transaction on Vehicular Technology*, VT-28(1).

Alvarez, L. (1996). *Automated Highway Systems: safe platooning and traffic flow control.* PhD thesis, Department of Mechanical Engineering, University of California at Berkeley.

Carbaugh, J. (1996). SmartPath regulation layer implementation: A user's guide. Master's thesis, Department of Mechanical Engineering, University of California at Berkeley.

Chiu, H. Y., Jr., G. B. S., and Jr., S. J. B. (1977). Vehicle follower control with variable-gains for short headway automated guideway transit systems. *Transactions of the ASME, Series G, Journal of Dynamic Systems, Measurement and Control*, 99(3).

Eskafi, F., Khorramabadi, D., and Varaiya, P. (1992). SmartPath: An automated highway system simulator. Technical Report UCB-ITS-92-3, University of California, Institue of Transportation Studies, Berkeley, CA.

Frankel, J., Alvarez, L., Horowitz, R., and Li, P. (1994). Robust platoon maneuvers for AVHS. Technical Report UCB-ITS-94-9, University of California, Institute of Transportation Studies, Berkeley, CA.

Godbole, D., Eskafi, F., and Singh, E. (1995). Design of an entry and exit maneuvers for AHS. *Proceedings of the 1995 American Control Conference.*

Hitchcock, A. (1994). Casualties in accidents occurring during split and merge maneuvers. Technical Report UCB-ITS-93-9, University of California, Institute of Transportation Studies, Berkeley, CA.

Hsu, A., Eskafi, F., Sachs, S., and Varaiya, P. (1991). The design of platoon maneuver protocols for IVHS. Technical Report UCB-ITS-91-6, University of California, Institue of Transportation Studies, Berkeley, CA.

Li, P., Alvarez, L., and Horowitz, R. (1997). AHS safe control laws for platoon leaders. To appear in the IEEE Control Systems Technology.

Lindesy, A. (1996). SmartPath implementation of communication protocols for a fault tolerant AHS design. To be appear as a PATH technical report.

Lygeros, J., Godbole, D., and Brouke, M. (1995). Design of an extended architecture for degraded modes of operation of IVHS. Technical Report UCB-ITS-95-3, University of California, Institue of Transportation Studies, Berkeley, CA.

Swaroop, D. (1994). *String Stability of Interconnected systems: An Application to Platooning in Automated Highway Systems*. PhD thesis, Department of Mechanical Engineering, University of California at Berkeley.

Varaiya, P. (1993). Smart cars on smart roads: Problems of control. *IEEE Transaction on Automatic Control*, AC-38(2).

Varaiya, P. and Shadlover, S. (1991). Sketch of an IVHS systems architecture. Technical Report UCB-ITS-PRR-91-3, University of California, Institue of Transportation Studies, Berkeley, CA.

Appendix A

Finishing Curve Derivation

A.1 Finishing curve for join/stoplight

In order to make a smooth transition from the flat portion of the safety curve to the final target state, where the spacing $\Delta x = \Delta x_d$ and the relative velocity $\Delta v = \dot{x}_{trail} - \dot{x}_{lead} = 0$, with zero acceleration a cubic spline is proposed of form

$$f(\Delta x) = \dot{x}_{trail} - \dot{x}_{lead} = a(\Delta x - \Delta x_d)^3 + b(\Delta x - \Delta x_d)^2 + c(\Delta x - \Delta x_d) + d\,, \tag{A.1}$$

where a, b, c, and d are coefficients to be determined. Eq. (A.1) has to satisfy the following boundary conditions

$$\begin{aligned} f(\Delta x_d) &= 0\,, & \text{(A.2)}\\ f'(\Delta x_d) &= 0\,, & \text{(A.3)}\\ f(\Delta x_d + \Delta x_{cubic}) &= \Delta v_{safe2}\,, & \text{(A.4)}\\ f'(\Delta x_d + \Delta x_{cubic}) &= 0\,, & \text{(A.5)} \end{aligned}$$

where

$f' = \frac{\partial f}{\partial \Delta x}$,
Δx_{cubic} is the length of the cubic spline,
$\Delta v_{safe2} = -(a_{max} + a_{min})d + v_{allow}$.

Substituting Eq. (A.2)-(A.5) into Eq. (A.1), we obtain that

$$\begin{aligned} c &= 0\,,\\ d &= 0\,. \end{aligned} \tag{A.6}$$

Coefficients a and b are given by

$$\begin{aligned} \begin{bmatrix} a \\ b \end{bmatrix} &= \begin{bmatrix} \Delta x_{cubic}^3 & \Delta x_{cubic}^2 \\ -3\Delta x_{cubic}^2 & 2\Delta x_{cubic} \end{bmatrix}^{-1} \begin{bmatrix} \Delta v_{safe2} \\ 0 \end{bmatrix} \\ &= -\frac{1}{\Delta x_{cubic}^4} \begin{bmatrix} 2\Delta x_{cubic} \\ -3\Delta x_{cubic}^2 \end{bmatrix} \Delta v_{safe2}\,. \end{aligned} \tag{A.7}$$

When the lead platoon is moving at constant speed, i.e. $\ddot{x}_{lead} = 0$, the acceleration needed for the trail car to travel along this trajectory is, from Eq. (3.1)

$$\begin{aligned} \ddot{x}_{trail} &= -f\frac{\partial f}{\partial \Delta x} \\ &= -(\Delta x - \Delta x_d)^3 \left[3a^2(\Delta x - \Delta x_d)^2 + 5ab(\Delta x - \Delta x_d) + 2b^2\right] . \end{aligned} \tag{A.8}$$

To ensure that the maximum braking required for the trail vehicle to travel along the trajectory without exceeding the comfort level, $-a_{com}$, the value of the extremum of Eq. (A.8) has to be bounded by $-a_{com}$. Equating the derivative of Eq. (A.8) to zero, that is

$$\frac{\partial \ddot{x}_{trail}}{\partial \Delta x} \mid_{v_{lead} = const} = -(\Delta x - \Delta x_d)^2 \left[15a^2(\Delta x - \Delta x_d)^2 + 20ab(\Delta x - \Delta x_d) + 6b^2\right] = 0 . \tag{A.9}$$

the location of the extremum of Eq.(A.9) in the range of $[\Delta x_d, \Delta x_d + \Delta x_{cubic}]$ is found to be

$$\Delta x_{ext} = \Delta x_d - 0.4558\frac{b}{a} . \tag{A.10}$$

The corresponding relative velocity Δv_{ext} is obtained from Eq. (A.1).

$$\Delta v_{ext} = (\beta^2 - \beta^3)\frac{b^3}{a^2}, \quad \text{where } \beta = -0.4558 . \tag{A.11}$$

Substitute Δx_{ext} in Eq. (A.10) into Eq. (A.8) and apply the constraint that $\min(\ddot{x}_{trail}(t)) \geq -a_{com}$ to obtain

$$0.0326\frac{b^5}{a^3} \geq -a_{com} . \tag{A.12}$$

Together with Eq. (A.7), the following inequality is obtained to select the length of the cubic spline.

$$\Delta x_{cubic} \geq 0.9902\frac{\Delta v_{safe2}^2}{a_{com}} \tag{A.13}$$

A.2 Finishing curve for frontdock

We proposed the use of a quadratic spline to finish the *frontdock* maneuver.

$$f(\Delta x_{faulty}) = \dot{x}_{trail} = a\Delta x_{faulty}^2 + b\Delta x_{faulty} + c \tag{A.14}$$

where $\Delta x_{faulty} = x_{trail} - x_{faulty}$ is the relative distance between the trail vehicle and the faulty vehicle. Since these two vehicles will be in contact at the end of the maneuver, the desired final spacing is zero.

The boundary conditions are given as follow

$$
\begin{aligned}
f(0) &= v_{faulty}\,, && \text{(A.15)}\\
f'(0) &= 0\,, && \text{(A.16)}\\
f(\Delta x_{spline}) &= v_{faulty} + (a_{max} + a_{min})d + \Delta v_{buff} && \text{(A.17)}\\
&\quad -\sqrt{2(a_{max} - a_{faulty})\Delta x_{spline}}\,,\\
f'(\Delta x_{spline}) &= -\frac{a_{max} - a_{faulty}}{\sqrt{2(a_{max} - a_{faulty})\Delta x_{spline}}}\,, && \text{(A.18)}
\end{aligned}
$$

where v_{faulty} is the velocity that the faulty vehicle maintains by executing the *constvel* maneuver when it requests a *frontdock*. Δx_{spline} is the length of the quadratic spline.

From Eqs. (A.15) and (A.16), we obtain that

$$
\begin{aligned}
b &= 0\,, && \text{(A.19)}\\
c &= v_{faulty}\,. && \text{(A.20)}
\end{aligned}
$$

Solving Eqs. (A.17) and (A.18), the parameter a and the length of the quadratic spline are given by

$$
a = -\frac{27(a_{max} - a_{faulty})^2}{64[(a_{max} + a_{min})d + \Delta v_{buff}]^3}\,, \qquad \text{(A.21)}
$$

$$
\Delta x_{spline} = \frac{8[(a_{max} + a_{min})d + \Delta v_{buff}]^2}{9(a_{max} - a_{faulty})}\,. \qquad \text{(A.22)}
$$